Investigating the Epoch of Galaxy Formation with Artificial Intelligence

by

Bradley Anthony Ward

A Thesis submitted to Cardiff University
for the degree of Doctor of Philosophy

December 2023

Abstract

" 5. Preliminary Pages 5.1 Each copy of the thesis must contain the following required pages: .1 a title page; **.2 a summary of no more than 300 words;** .3 a list of contents, which includes the page number for each chapter and sub-division listed; .4 acknowledgments, where this is an expectation of your sponsor "
as taken from Submission-and-Presentation-of-Research-Degree-Theses.pdf — Policy on the Submission and Presentation of Research Degree Theses – v 5.0 – Date of Effect 01.08.2022 – accessed 22/09/2022

Publications

Preface

Keep in mind the wise words of Louise Winter (PGR Admin School of PHYSX (as of 2022)) "if you have material that has been published in journals in your thesis you are advised to seek permission from the relevant journal to publish in your thesis for the final version to be published on ORCA – take a little time to read this page. If you are uncertain about Copyright you should contact Copyright@cardiff.ac.uk as we are not experts on copyright. "
`https://intranet.cardiff.ac.uk/students/study/postgraduate-research-support/`
`thesis-and-examinations/submitting-your-thesis/copyright-and-your-ethesis`

First Author Publications

authors, et al. year; *Title*, Submitted to MNRAS

Co-Author Publications

, In Prep

Contents

"A dedication quote/sentence"

Acknowledgements

"A quote"

By whom *From what source*

Funding Bodies and Affiliations

Insert thanks to funding bodies, and affiliations (e.g. partner company, CDT, governments, University funders, grants/awards, etc. . . .) There are no strict rules on logos here — use at your discretion.

Personal Thanks

Insert personal thanks, e.g. supervisors, friends, family, colleagues. Keep it proffesional.
"8. Acknowledgements/Dedications 8.1 It is understandable that you will have benefitted from the support of family, friends and peers whilst undertaking your studies and you may wish to express your thanks in an acknowledgements/dedication section of your thesis. If you choose to do this, you should be mindful of the nature and tone of your comments as they may be read widely, including by future employers, funders or other colleagues. 8.2 For data protection purposes, you should not include any private personal details or other confidential information about yourself or others in the acknowledgements section or elsewhere in the thesis." — University (`https://intranet.cardiff.ac.uk/students/study/postgraduate-research-support/thesis-and-examinat` `preparing-your-thesis`) Submission-and-Presentation-of-Research-Degree-Theses V5.0 September 2022

x

Chapter 1

Introduction

1.1 A title

Chapter 2

Herschel-ATLAS Data Release III

2.1 The Herschel-ATLAS

The *Herschel* Astrophysical Terahertz Large Area Survey (H-ATLAS; Eales et al. 2010) was the largest open-time sub-mm survey carried out with *Herschel*. The survey was observed across five photometric bands using two instruments onboard the *Herschel Space Observatory*: the Photodetector Array Camera (PACS, Poglitsch et al. 2010) at 100 and 160 µm, and the Spectral and Photometric Imaging Receiver (SPIRE, Griffin et al. 2010) at 250, 350 and 500 µm. Compared to the first SMGs (Assumption: I have already described SMGs and their initial discovery in the 90s.) detected using SCUBA at 850 µm(Smail et al. 1997; Barger et al. 1998; Hughes et al. 1998), the PACS and SPIRE wavebands span the peak of the infrared spectrum for low redshift (z < 1) galaxies. Their intrinsic brightness at the SPIRE wavelengths makes their detection in the thousands more achievable.

The complete survey covers $\sim 660 \deg^2$, split into three regions located to avoid emission from Galactic dust and to utilize complimentary spectroscopic surveys including the Sloan Digital Sky Survey (SDSS, York et al. 2000), the 2df Galaxy Redshift Survey (2dfGRS, Colless et al. 2001) and the Galaxy and Mass Assembly (GAMA, Driver et al. 2009). The North Galactic Pole (NGP) region covers $\sim 180 \deg^2$ of the northern sky, centered at R.A 13^h18^m and declination $+29°13'$ (J2000); three equatorial fields, located at approximately R.A 9^h, 12^h and 15^h coinciding with the GAMA survey (henceforth named GAMA9, GAMA12 and GAMA15 fields), each with an area of approximately $54 \deg^2$, and the South Galactic Pole (SGP) region, centered at R.A 0^h6^m and declination -32°44' (J2000) with an area of $\sim 318 \deg^2$.

### 2.1.1 Detecting Submillimeter Sources on Herschel Images

Due to [...] sub-mm images suffer from two types of noise; instrumental noise [...] and confusion noise which is highly correlated between pixels, most of its contribution coming from the blending

together of faint sources. Source confusion is of particular importance to sub-mm surveys [...]. The result of combining instrumental noise with confusion noise is that almost all sources in the Herschel images are unresolved and the optimum filter for detecting these unresolved sources is no longer the point spread function (PSF). Consider a *Herschel* map in which there is only one source of noise: an image with instrumental noise but no confusion noise (i.e. there is only one point source and no fainter, confusing sources), the optimal detection of this source is obtained by convolving the image with the PSF of the instrument. On the other hand, a map with no instrumental noise, but many confused point sources would be optimally detected with its best signal to noise ratio (SNR) by taking the Fourier transform of the image, dividing by the Fourier transform of the PSF and taking the inverse Fourier transform to obtain a perfect deconvolution of the original map (Reference). For images that have a variable ratio of instrumental to confusion noise like the *Herschel* images of H-ATLAS, Chapin et al, 2011 showed that a convolving function or "matched filter" can be calculated to provide the maximum SNR for an unresolved source.

To detect H-ATLAS sources from the 250 µmmaps using a matched filter (the 250 µmband is the most sensitive of the SPIRE bands and given the lower sensitivity of the PACS instrument, all sources detected on the PACS images would also be detected on the SPIRE 250 µmimage), Maddox et al, 2020 developed a source detection algorithm called the Multi-band Algorithm for Source Detection and eXtraction (MADX). The MADX algorithm works in the following way. Firstly, Galactic dust emission is removed from the images using Nebuliser. Next, the images are convolved with the matched filter (which needs description). The variance map is created by convolving the map of variance in instrumental noise with the matched filter and adding the confusion noise. It is from this map that the SNR of a detected source is determined. The same process is repeated with the 350 and 500 µmmaps and interpolated to the same pixel scale as the 250 µmmaps. The detection map used to extract sources is then created from a weighted average of the three SPIRE maps, however, due to the smaller PSF at 250 µmwhich leads to more accurate positions and the increased number of sources when using the 250 µmmaps, zero weighting is given to the 350 and 500 µmimages. This has the effect of making the detection map the same as the 250µmmap.

Sources are identified by peak values $> 2.5\sigma$ in the filtered detection map. Their positions are estimated by fitting a Gaussian to the nearest pixels surrounding the location of the peak. The source is extracted in the other *Herschel* wavebands at the 250 µmposition. Due to the high levels of confusion and high source density on the SPIRE maps, the flux density estimates in each band can be biased by blending with other sources. The MADX algorithm negates some of this problem by ordering the sources by their flux density estimates and iteratively fitting and removing a point source from the position of each source, starting with the brightest. The new estimates of the flux densities are then not influenced by contamination from brighter sources.

The catalogue of point sources provided by H-ATLAS come from the extraction of point sources
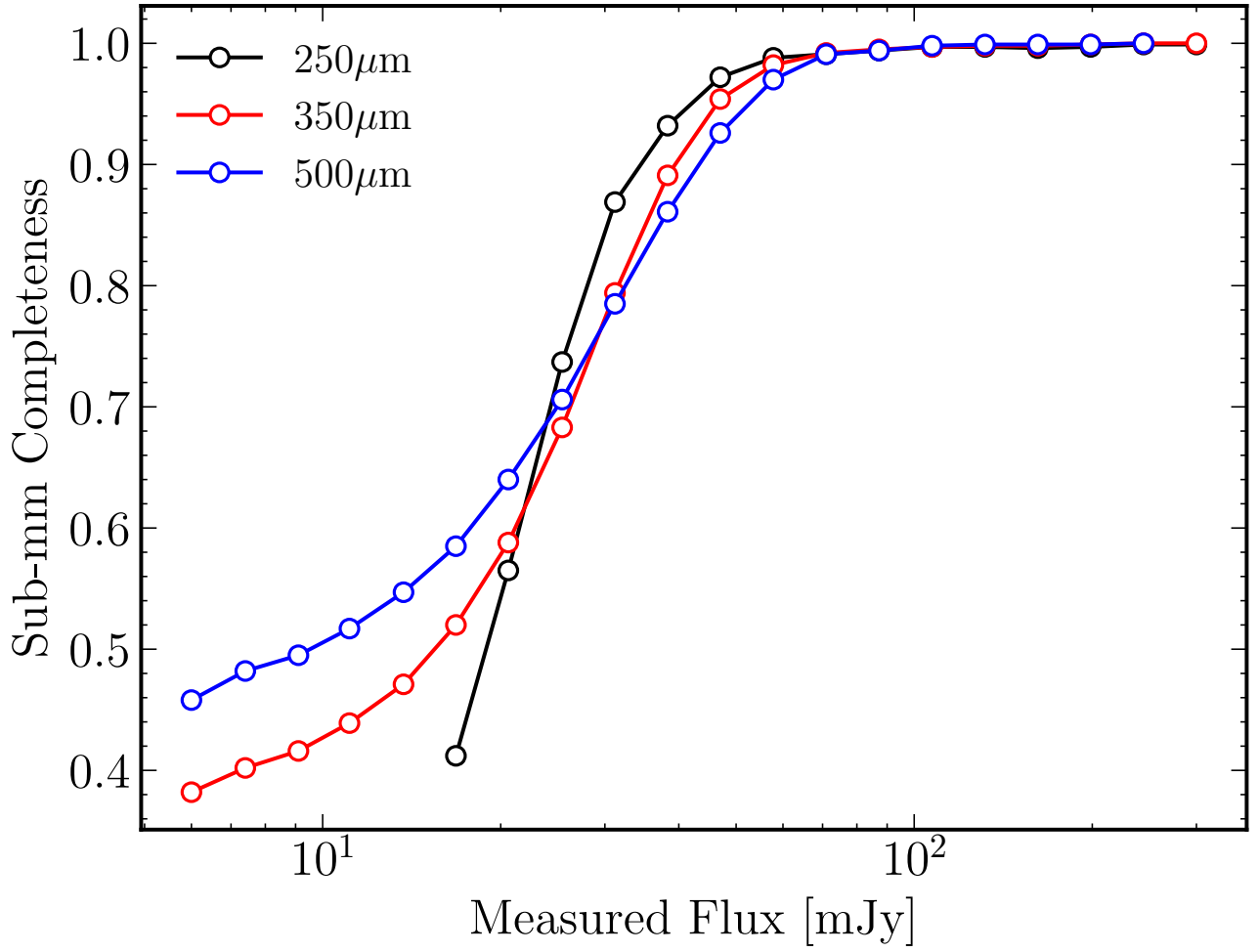
Figure 2.1. Caption

using MADX applied to the SPIRE images of the NGP, SGP and GAMA fields. The final sources list is reduced to those sources with SNR > 4 in any of the SPIRE bands. While the detection method suggests that we may miss sources that are faint at 250 μmbut bright at 350 or 500 μm, due to the weighting of the three images, cataloguing all sources with SNR > 4 in any of the SPIRE bands means that the catalogues are reasonably complete in all bands. The completeness of the sub-mm catalogues as a function of the measured flux density of a source as estimated by Valiante et al. 2016 is illustrated in Figure 2.1.

2.1.2   Data Releases of the H-ATLAS

The first public data release (DR1) of H-ATLAS covered the three equatorial GAMA fields, which span approximately 25 % of the total survey area. These fields benefit from multiwavelength coverage from GAMA, SDSS, 2dF, the Galaxy Evolution Explorer (GALEX, Martin et al. 2005), the UKIRT Infrared Deep Sky Survey – Large Area Survey (UKIDSS-LAS, Lawrence et al. 2007),

the Wide-field Infrared Survery Explorer (WISE, Wright et al. 2010), the VISTA Kilo-degree Infrared Galaxy survey (VIKING, Edge et al. 2013) and the Kilo-Degree Survey (KiDS, de Jong et al. 2013).

Sources are provided with DR1 if they are detected above the 2.5σ detection limit on the $250\,\mu m$map and have measured flux densities greater than the 4σ flux density limits in one of the three SPIRE bands (29.6 mJy, 37.6 mJy or 40.8mJy at 250, 350 and 500 µm). Across the three fields there are a total of 113,995, 46,209 and 11,011 sources detected at $> 4\sigma$ at 250, 350 and 500 µmas well as detections for 4,650 and 5,685 sources at $> 3\sigma$ at 100 and 160 µm(Valiante et al. 2016). Following the release of the sub-mm sources detected in the GAMA fields, Bourne et al. 2016 used the Likelihood Ratio (LR) method (Section 2.2.1) to identify potential optical counterparts to the 113,995 sources with $SNR_{250} > 4$ from SDSS. Sources with $SNR_{250} < 4$ that were detected by their 350 or 500 µmflux densities were omitted from the matching since these sources have sub-mm colours suggesting a high redshift, and are the most likely sources to be misidentified by SDSS due to the increased probability of chance alignments or gravitational lensing along the line of sight (Negrello et al. 2010; Pearson et al. 2013; Bourne et al. 2014). Description of Bourne+2016 main findings.

The second public data release (DR2) covered the NGP and SGP, two large fields that together form $\sim 75\,\%$ of the total survey area. The NGP was covered in the optical by the SDSS and in the near-infrared by UKIDSS-LAS. Moreover, a small area of $25.93\,\mathrm{deg}^2$ within the NGP was also observed by a deeper K-band survey by the H-ATLAS team using UKIRT (limiting magnitude of K < 19.40 compared to K < 18.69 for UKIDSS-LAS). The SGP is the largest field (approximately half the survey area of H-ATLAS) and was covered by the 2dF spectroscopic survey, KiDS in four optical bands (u, g, r and i) and VIKING in five near-infrared bands (Z, Y, J, H and K_s). Given that sub-mm sources are only extracted from areas of the *Herschel* maps that have at least two obsersations from the SPIRE instrument, the DR2 catalogues includes sources from the map area reduced by the masking of single *Herschel* scans. The mask reduces the area covered by the NGP point source catalogue to $177.1\,\mathrm{deg}^2$ and the SGP to $303.4\,\mathrm{deg}^2$. As with DR1, sources are included if they are detected on the $250\,\mu m$map above the 2.5σ detection limit by the MADX algorithm and surpass at least one of the 4σ flux density limits at the SPIRE wavelengths.

2.2 Identifying Multiwavelength Counterparts to Herschel Sources

2.2.1 The Likelihood Ratio Method

Chapter 3

Conclusion

"A quote"

By whom *From what source*

Appendix A

An Appendix

A.1   An Appendix

Bibliography

Barger A. J., Cowie L. L., Sanders D. B., Fulton E., Taniguchi Y., Sato Y., Kawara K., Okuda H., 1998, *Nature*, 394, 248

Bourne N., et al., 2014, *MNRAS*, 444, 1884

Bourne N., et al., 2016, *MNRAS*, 462, 1714

Colless M., et al., 2001, *MNRAS*, 328, 1039

Driver S. P., et al., 2009, Astronomy and Geophysics, 50, 5.12

Eales S., et al., 2010, *PASP*, 122, 499

Edge A., Sutherland W., Kuijken K., Driver S., McMahon R., Eales S., Emerson J. P., 2013, The Messenger, 154, 32

Griffin M. J., et al., 2010, *A&A*, 518, L3

Hughes D. H., et al., 1998, *Nature*, 394, 241

Lawrence A., et al., 2007, *MNRAS*, 379, 1599

Martin D. C., et al., 2005, *ApJ*, 619, L1

Negrello M., et al., 2010, Science, 330, 800

Pearson E. A., et al., 2013, *MNRAS*, 435, 2753

Poglitsch A., et al., 2010, *A&A*, 518, L2

Smail I., Ivison R. J., Blain A. W., 1997, *ApJ*, 490, L5

Valiante E., et al., 2016, *MNRAS*, 462, 3146

Wright E. L., et al., 2010, *AJ*, 140, 1868

York D. G., et al., 2000, *AJ*, 120, 1579

de Jong J. T. A., Verdoes Kleijn G. A., Kuijken K. H., Valentijn E. A., 2013, Experimental
Astronomy, 35, 25